Robotica: (2019) volume 37, pp. 1987–1997. © Cambridge University Press 2019
doi:10.1017/S0263574719000390

Using One Strain Gauge Bridge to Detect Gait Events for a Robotic Prosthesis

Yanggang Feng†, ‡ and Qining Wang†, ‡, ¶*

†*The Robotics Research Group, College of Engineering, Peking University, Beijing 100871, China*
‡*Beijing Innovation Center for Engineering Science and Advanced Technology (BIC-ESAT), Peking University, Beijing 100871, China*
¶*Beijing Engineering Research Center of Intelligent Rehabilitation Engineering, Beijing 100871, China*

(Accepted March 3, 2019. First published online: April 1, 2019)

SUMMARY
For a real-time robotic prosthetic control, gait event detection plays an important role. In this paper, one novel sensor was proposed to realize gait event detection. The sensor includes one strain gauge bridge, which can reflect the entire deformation of carbon-fiber footplate on a robotic prosthesis. Three unilateral transtibial amputees participated in the experiments. Experimental results show that using the proposed sensor method, gait event detection (stance phase and swing phase) accuracy is approximately 100%. Based on the detected gait events, three locomotion modes (sit, stand, and walk) and the corresponding transition modes could be determined. Difference between different gait event detection systems was further conducted.

KEYWORDS: Man–Machine Systems; Mechatronic Systems; Sensor or Actuator Design; Prosthesis; Human Biomechanics

1. Introduction

With the improvement of life quality, lower-limb amputees increase their demand for prostheses. Most existing commercial lower-limb prostheses are passive with rigid ankle joints, which may result in the gait asymmetry and the high metabolic cost.[1,2] To improve the gait symmetry and decrease the metabolic cost, increasing efforts have been made on robotic prostheses instead of passive prostheses, for example, refs. [3–12]. For the prosthetic control, challenges in gait event detection still exist and several approaches are proposed to deal with the challenges.

Based on algorithm complexity, the algorithms of gait event detection can be divided into two categories. One category depends on designed models. For example, an adaptive-oscillators-based method using noncontact capacitive sensing was used to detect gait events.[13] Kyoungchul *et al.* proposed a fuzzy-logic-based approach to detect gait events smoothly and continuously.[14] The proposed algorithm was implemented by using signals from sensor-embedded shoes called smart shoes. In addition, machine learning algorithm was widely used in gait event detection. Mannini *et al.* presented an approach to the online implementation of a gait event detector based on a hidden Markov model, and gait events were detected using a uniaxial gyro.[15] There are still challenges when the model-based algorithms are applied to amputees for realizing the real-time prosthetic control. Moreover, model generalization is another issue required to be considered. Those pattern-recognition-based methods need training process and labeled information, which may lead to the high uncertainty when encounters the untrained gait patterns.

The other category uses threshold judgement instead of designed models. For example, Cherelle *et al.* utilized two force sensing resistors placed at foot sole (heel and toes) in order to sense the

* Corresponding author. E-mail: qiningwang@pku.edu.cn

https://doi.org/10.1017/S0263574719000390 Published online by Cambridge University Press

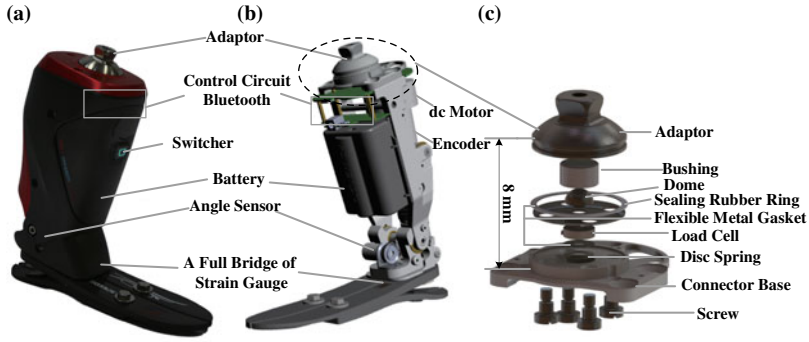


Fig. 1. Robotic transtibial prosthesis prototype: (a) Appearance. (b) Internal mechanical structure. The electric control system includes sensor subsystem, processing subsystem, and actuator subsystem. The sensor subsystem consists of a load cell, a full bridge of strain gauge, an angle sensor, an encoder (motor), and a switcher. The processing system utilized the STM32F103 processor. The actuator subsystem utilizes a three-phase motor predriver (A4931, Allegro LLC.) to actuate the EC 45 motor (50 W, Maxon Inc.). The mechanical structure is composed of a three-bar model. To analyze the data, the Bluetooth is utilized to send data to a computer. (c) Exploded assembly view of a load cell sensor. To install the load cell sensor, the corresponding mechanical structure is designed, whose net height and weight are 8 mm and 90 g, respectively.

ground reaction force as the important triggers. These triggers can be used to detect four gait phases (heel strike to foot flat, foot flat to heel off, heel off to toe off, and swing) .[9] For different gait phases, the corresponding control strategies were adopted. Note that this foot sole is separated from the prosthesis and not integrated into the prosthesis. Au *et al.* integrated sensors into the prosthesis and utilized six capacitive force transducers to detect the heel contact and toe contact .[7] The heel and toe contact information combining ankle angle, ankle torque, and state duration was used to detect six phases (controlled plantar flexion, controlled dorsiflexion, powered plantar flexion, and swing 1–3). Sup *et al.* proposed a sensorized foot including two full bridges of strain gauges to detect ball of foot contact and heel strike.[6] Ankle angle and knee velocity combing the signals from a sensorized foot were used to detect five gait phases (early stance, middle stance, late stance, swing flexion, and swing extension).

In our previous studies, a uniaxial load cell (height: 32 mm; weight: 138 g (including the pyramid connector)) was utilized to detect gait events for a lightweight prosthesis (1.3 kg without a battery), which shows an improved performance on terrain adaptation.[11,16,17] In addition, we further improved the prosthetic power without increasing too much weight (1.75 kg without a battery), and a six-axis torque/force sensor (height: 45 mm; weight: 190 g (including the pyramid connector)) was utilized to detect gait events. Although the sensors installed between adaptor and prosthesis can detect gait events, such installation would result in increasing weight and height. In this paper, we utilized one full bridge of strain gauge to measure the deformation during stance phase to detect gait events. Gait event includes rearfoot strike (RS), rearfoot-to-forefoot strike (R2FS), forefoot strike (FS), and toe off (TO). To meet the control requirement, based on gait events, two gait phases (stance phase and swing phase) and three locomotion modes (sit, stand, and walk) are determined.

This paper is organized as follows. Section 1 introduces the proposed prosthetic prototype. Section 3 describes prosthetic control strategy. Section 4 states experimental methods. Experimental results are shown in Section 5. Finally, Sections 6 and 7 show discussion and conclusion, respectively.

2. Robotic Prosthesis

In our previous study, we proposed a prosthesis and a damping control strategy during stance phase, which showed satisfactory performance on terrain adaptation.[11] In this paper, the prosthesis on gait phase detection and wearing comfort were improved, shown in Fig. 1.

For the current version, the electrical control system consisted of the sensor subsystem, the processing subsystem, and the actuator subsystem. In this paper, to compare with the signal difference between a load cell sensor and a full bridge of strain gauge sensor, a load cell sensor was still retained as the reference. Therefore, the sensor subsystem consisted of a load cell, a full bridge of strain gauge, an angle sensor, a motor encoder, and a switcher (see Fig. 1(a–b)). An angle sensor was used for ankle joint measurement. A switcher was designed to turn on/off the power supply. The processing system

https://doi.org/10.1017/S0263574719000390 Published online by Cambridge University Press

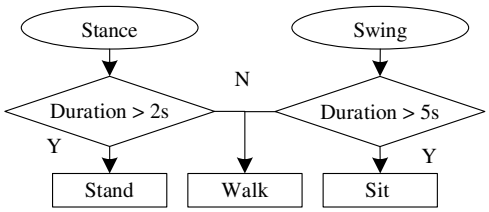


Fig. 2. Mode recognition.

utilized the STM32F103 processor to collect the relevant sensor data and send commands to the actuator. The actuator subsystem utilizes a three-phase motor predriver (A4931, Allegro LLC.) to actuate the EC 45 motor (50 W, Maxon Inc.). The mechanical structure was simplified as a three-bar model, and detailed mechanical parameters were mentioned in our previous study.[17] In addition, to analyze the data, the data were sent to a computer by Bluetooth. Sending frequency was 100 Hz and the baud rate was 57,600 bit/s. Note that to install the load cell sensor, the corresponding mechanical structure, whose net height and weight were 8 mm and 90 g, respectively, was designed (see Fig. 1(c)). Through bushing and dome, the lateral force would produce a vertical pressure on the flexible metal gasket. The flexible metal gasket would deform and had the pressure on the load cell sensor. When the load cell sensor was not exerted by any force, the disc spring would get the load cell sensor to return to the initial position.

Compared with the previous prosthesis,[11] in this paper, we improved the prototype as follows (see Fig. 1). First, the battery installation was changed as an embedded one. Second, the switcher was added instead of plugging in/out the battery. Third, a full bridge of strain gauge sensor could sense the footplate deformation in both directions, and local deformation could reflect the entire deformation of carbon-fiber footplate during stance phase (see Fig. 3).

3. Control Strategy

Two-level controllers were applied as the real-time prosthetic control strategy. Based on the determined gait events, the high-level controller was designed to realize gait phase estimation (stance phase and swing phase) and mode recognition (sit, stand, and walk). For different gait phases and modes, the low-level controller was designed to implement different control strategies.

3.1. High-level controller: gait phase estimation and mode recognition

The high-level controller utilized the signals of strain gauge bridge and the state duration to distinguish different gait phases (stance phase and swing phase) and modes (stand, sit, and walk), shown in Fig. 2.

Recently, we proposed a lightweight prosthesis which could adapt to different terrains.[11] For this prosthesis, the control system was required to distinguish the stance phase and swing phase. The distinguishing method replied on the threshold from the load cell sensor. However, increasing the load cell sensor will increase by 90 g weight and 2 cm height. Increasing the prosthetic weight may increase the metabolic cost and cause some gait asymmetry for amputees,[1,2] and increasing the prosthetic height will result in that some transtibial amputees with the too long residuals cannot wear.

In this paper, instead of using the load cell sensor to distinguish stance phase and swing phase, we utilized one full bridge of strain gauge sensor to measure the carbon-fiber footplate deformation during stance phase. The principle of measuring the deformation by a strain gauge sensor is shown in Fig. 3. In Fig. 3, the deformation direction between FS and RS is different. Therefore, the signal characteristics of the strain gauge sensor between FS (negative value) and RS (positive value) are different. However, when the transition occurs from RS to FS during stance phase, the signal characteristics are similar to the signal during swing phase. Therefore, the strain gauge sensor cannot rely on the threshold to estimate stance phase and swing phase as the load cell sensor does.

In this paper, we proposed a method using one full bridge of strain gauge sensor to distinguish the stance phase and the swing phase, shown in Fig. 4. In this method, the current gait phase relies on not only the current state but also the previous flag and state duration. The flag types include RS, R2FS, FS, and swing. Based on the current gait state and state duration, three modes are determined. First,

https://doi.org/10.1017/S0263574719000390 Published online by Cambridge University Press

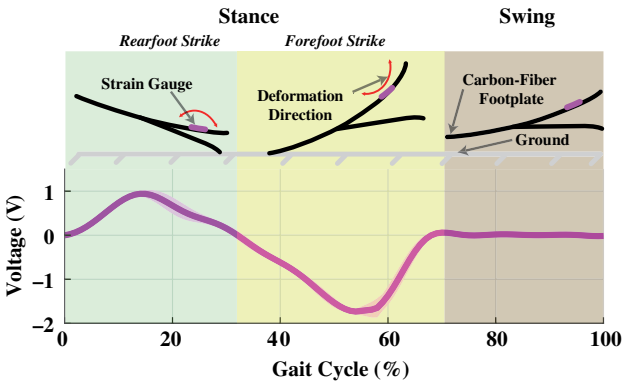


Fig. 3. The principle of a full bridge of strain gauge sensor. The red arrow refers to deformation direction of carbon-fiber footplate and the red line refers to the strain gauge sensor. When the carbon-fiber footplate touches the ground, the footplate could be regarded as a cantilever beam. When FS occurs, the deformation direction of carbon-fiber footplate is upward. When RS occurs, the deformation direction of carbon-fiber footplate is downward. When the carbon-fiber footplate leaves off the ground, this state reflects initial state of carbon-fiber footplate without the extra force. The purple line and shaded area refer to the mean and standard deviation of strain gauge signals, respectively.

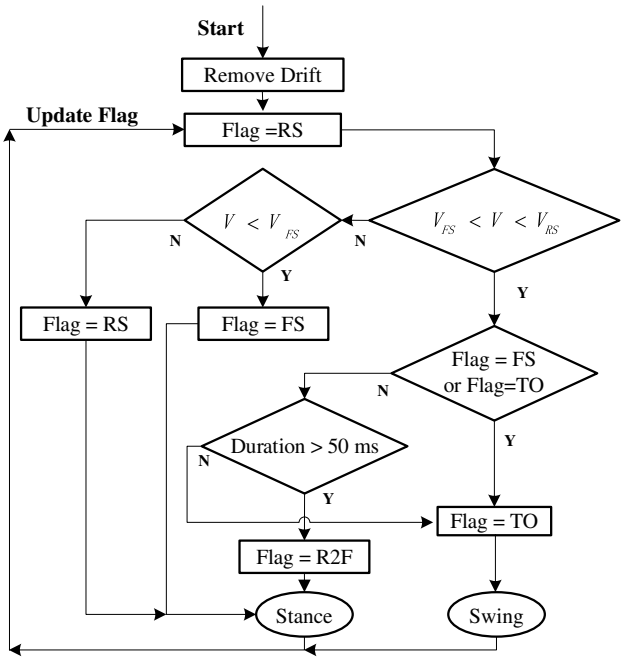


Fig. 4. Distinguish the stance phase and the swing phase. V refers to the value from the full bridge of strain gauge. V_{RS} and V_{FS} refer to RS threshold and FS threshold, respectively. The abbreviations RS, R2RS, FS, and TO refer to RS, R2FS, FS, and TO, respectively.

the control system determines the current state (swing phase or stance phase). Second, if the current phase is swing phase and phase duration is over 5 s, the current mode is determined as sit mode. If the current phase is stance phase and the phase duration is over 2 s, the current mode is determined as stand mode. Otherwise, the current mode is determined as walk mode. The duration selection makes a trade-off between the long delay and stable recognition.

3.2. Low-level controller: damping control and position control

The motor controller was designed to implement damping control and position control based on current state (gait phase and mode). For damping control and position control, the motor works in the passive damping state and the active motion state, respectively.

https://doi.org/10.1017/S0263574719000390 Published online by Cambridge University Press

Table I. Damping control parameters for different modes.

Mode	θ_0(°)	θ_{d1} (°)	s_1	θ_{d2} (°)	s_2	k_{per}(%)
Walk	0	−3	0.5	5	0.25	70
Stand	0	−3	0.5	5	0.25	100
Sit	0	−3	0.5	5	0.25	0

3.2.1. Damping control. Different from the active magnetic damper, we used a method to realize real-time prosthetic damping control.[11] The methods can result in the equal braking torque τ_{eb} due to the different duty cycle (D) of the Pulse Width Modulation (PWM) signal and the equation is as follows:

$$\tau_{eb} = k_{eb} D n. \tag{1}$$

where k_{eb} is the proportionality coefficient in the unit of Nm/rpm and n is the motor speed in the unit of rpm. As the duty cycle D determines the relationship between the torque and the speed, it can be regarded as the damping coefficient. The controller switches between the damping function of the controlled plantar flexion (D_1) and the damping function of the controlled dorsiflexion (D_2) according to the angular rate $\dot{\theta}$,

$$\begin{aligned} D &= \begin{cases} k_{per} D_1, & \dot{\theta} < 0 \\ k_{per} D_2, & \dot{\theta} \geqslant 0 \end{cases} \\ D_1 &= 1 - 0.5(\tanh(s_1(\theta - \theta_{d1})) + 1) \\ D_2 &= 0.5(\tanh(s_2(\theta - \theta_{d2})) + 1) \end{aligned} \tag{2}$$

where k_{per} the percentage of the duty cycle for the different modes (sit, stand, and walk), θ_{d1} is the threshold plantar flexion angle, θ is the current joint angle, s_1 is the sensitivity factor that decides the slope of the function and the resulted D_1 is the duty cycle of the PWM signal that controls the motor terminal short, s_2 is the sensitivity factor that decides the slope of the function and the resulted D_2 is the duty cycle of the PWM signal that controls the motor terminal short, and θ_{d2} is the threshold dorsiflexion angle. Note that $\dot{\theta} < 0$ and $\dot{\theta} > 0$ refer to plantar flexion and dorsiflexion, respectively.

3.2.2. Position control. For the active motion state, the Proportional-Derivative (PD) controller was developed in motor control. The principle of PD controller is as follows:

$$D_a = k_p(\theta_0 - \theta) + k_d(\dot{\theta_0} - \dot{\theta}) \tag{3}$$

where D_a is the active controller output for motor driver, k_p and k_d are predefined constants, and θ_0 and $\dot{\theta_0}$ are the desired equilibrium angle and desired angular velocity of swing, respectively. In this paper, k_p and k_d are set to $6\%/degrees$ and $2\%/(degrees/s)$, respectively.

3.2.3. Application. For different gait phases and modes, different low-level motor controllers are developed as follows. Note that stance phase in sit mode and the swing phase in stance mode do not exist in our proposed control strategy. Detailed control parameters for different modes can refer to (Table I).

- *Walk Mode*. In walk mode, the gait phase was divided into stance phase and swing phase. During stance phase in walk mode, the prosthesis is required to adapt to different terrains, and thus the passive damping controller was applied to the prosthesis. During stance phase, the active motion controller (PD controller) was utilized to get the prosthesis return to the equilibrium position.
- *Stand Mode*. In stand mode, passive damping control was also utilized to realize stand firmly. However, compared with the walk mode, the braking torque was larger for stand mode. Parameter k_{per} was changed as 100% to achieve a larger braking torque.
- *Sit Mode*. In stand mode, damping control was still utilized to realize the prosthetic-free movement. Compared with the walk mode and stand mode, the braking torque is smallest. We change parameter k_{per} to 0 % to achieve the desired-free movement.

https://doi.org/10.1017/S0263574719000390 Published online by Cambridge University Press

Table II. Detailed information of the amputee subjects.

Subject	Age	Weight (kg)	Height (cm)	Gender	Amputation leg	Amputation years	Residual limb ratio
1	55	70	170	Male	Left	15	40 %
2	54	82	170	Male	Left	8	32 %
3	35	65	172	Male	Left	19	31 %

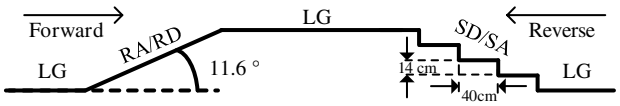


Fig. 5. The diagrammatic drawing of different terrains. The abbreviations LG, RA/RD, and SD/SA stand for level ground, ramp ascent/ramp descent, and stair descent/stair ascent, respectively. The slope angle is 11.9°. The length and width of the stairs are 40 and 14 cm, respectively.

4. Experimental Methods

4.1. Subjects and experimental environment

Three unilateral transtibial amputees volunteered to participate in the experiments and signed the prior written consent. The experiments were approved by the Local Ethics Committee of Peking University. Detailed information about subjects is presented in Table II. Both signals from a load cell sensor and a full bridge of strain gauge sensor were processed by a first-order low-pass hardware filter with 1 KHz cut-off frequency, and then encoded by a 12-bit Analog-to-Digital Converter. The sampling frequency is 100 Hz. The subjects were asked to walk at five different terrains: level ground (LG), ramp ascent (RA), ramp descent (RD), stair ascent (SA), and stair descent (SD), shown in Fig. 5. The slope angle is 11.9°. The length and width of the stairs are 40 cm and 14 cm, respectively.

4.2. Experiment protocol

4.2.1. Terrain experiment. Before experiments, to adapt to the robotic prosthesis, the subjects walked at least for 20 min. The subjected were encouraged to walk at their most suitable speed and step length. Based on the preference of the subjects, the control parameters were adjusted and the most suitable step length for each subject was recorded by the landmarks. To automatically analyze the terrains, during the experiments, the subjects were asked to walk at the fixed step length (i.e. follow the landmarks). The subjects were asked to ambulate in two directions. For the forward ambulation direction, the subjects began to walk on LG, and then RA, LG, and SD, and ended at LG (from left to right in Fig. 5). For the reverse ambulation direction, the subjects began to walk on LG, and then SA, LG, and RD, and ended at LG (from right to left in Fig. 5). The forward and reverse direction ambulation was a trial. For each subject, 30 trials were done. Individual walking preference in the same terrain shows the difference, and the individual experimental results are presented separately. In addition, for each subject, the walking preference at different terrains is different, and thus the experimental results for different terrains are presented separately. To compare with the difference between the load cell sensor and strain gauge sensor, all experimental data were divided by the mean value of the first peak signal on LG walking as the normalized data.

4.2.2. Mode and transition experiment. In this paper, to study the performance of the full bridge of strain gauge sensor on three modes and transitions between three modes, the experiment on three modes and six transitions between three modes were done for subject 2. To compare the difference between two sensors, (load cell and strain gauge), the synchronous signal of the load cell sensor was collected. To verify the experimental results, the modes and transition states were recorded by the video. This experiment is divided into three aspects as follows:

- *Sit-Stand-Sit*. Subject 2 was asked to sit down for about 10 s, and then stand for about 10 s, at last, sit down for about 10 s.

https://doi.org/10.1017/S0263574719000390 Published online by Cambridge University Press

Table III. Gait event recognition results (three participants).

	LG	RA	RD	SA	SD
Total gait events	900	450	450	270	270
Detected gait events	899	450	450	270	270
Undetected gait events	1	0	0	0	0
Total recognition accuracy (%)	99.9	100	100	100	100

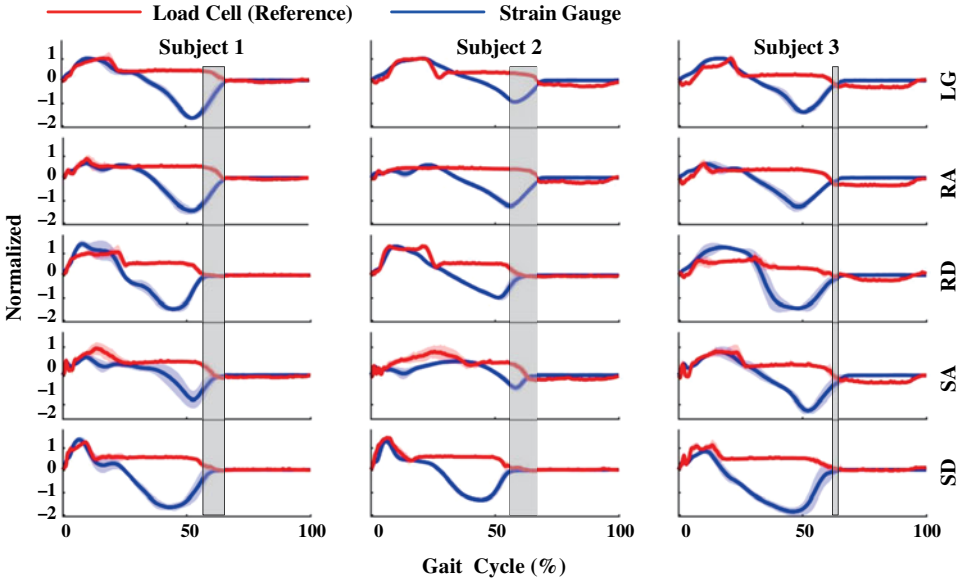


Fig. 6. Experimental results for different terrains. The red line and shade represent the signals from the load cell sensor, and the blue line and shade indicates the signals from the strain gauge sensor. The abbreviations LG, RA, RD, SA, and SD stand for level ground, ramp ascent, ramp descent, stair ascent, and stair descent, respectively. Gait cycle begins at heel strike and ends at the next heel strike. The gray-shaded area shows the transition between stance phase and swing phase. At the left shaded area, the gait phase is stance phase, and at the right shaded area, the gait phase is swing phase.

- *Stand-Walk-Stand*. Subject 2 stood for about 10 s, and then walked three steps (prosthetic side), at last, stopped and stand for about 10 s.
- *Sit-Walk-Sit*. Subject 2 sat down for about 10 s, and then stood as soon as possible to walk three steps (prosthetic side), at last, stopped as soon as possible and sat down for about 10 s.

5. Results

5.1. Terrains

For different terrains, gait event detection results are shown in Fig. 6. One whole gait cycle begins at heel strike and ends at the next heel strike. The shaded area represents transition area (stance-to-swing). A load cell sensor was utilized to measure the interaction force as the reference signal (Fig. 6). As shown in Fig. 6, swing phase and stance phase could be distinguished clearly. During swing phase, the values of both the sensors (strain gauge and load cell) fluctuate around zero. The signal difference between load cell sensor and strain gauge sensor occurs at stance phase. For the load cell sensor, the values are always greater than zero during stance phase. However, for the strain gauge sensor, the values are first greater than zero and then decrease to blow than zero. This is due to that the strain gauge bridge could detect not only RS but also FS. For RS and FS, the deformation direction of carbon-fiber footplate is different, and thus the resulted values are different (positive and negative). For each terrain, the recognition accuracy of gait events is approaching 100%, shown in Table III. It means that the sensor system that we proposed has the capability of replacing the load cell sensor to detect stance phase and swing phase.

https://doi.org/10.1017/S0263574719000390 Published online by Cambridge University Press

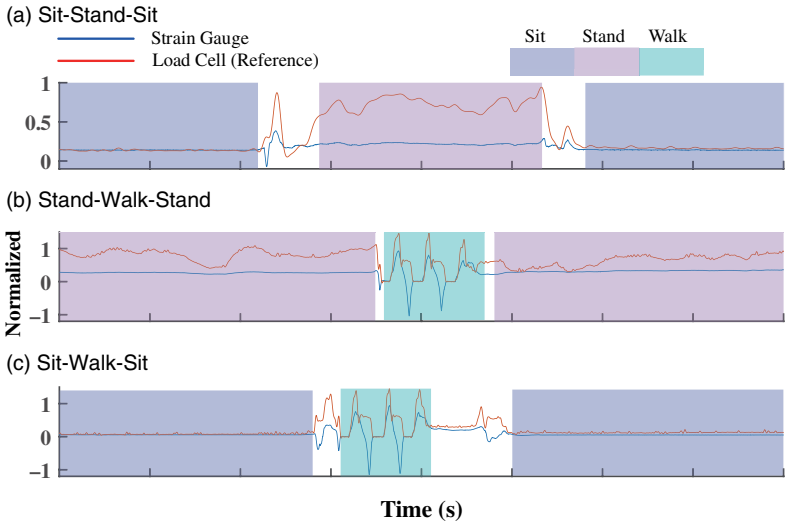


Fig. 7. Mode-transition experiments of subject 2. (a) Sit-stand-sit mode. (b) Stand-walk-stand mode. (c) Sit-walk-sit mode. The red line represents the signals from the load cell sensor and the blue line indicates the signals from the strain gauge sensor. The purple-, magenta-, and cyan-shaded area refer to sit mode, stand mode, and walk mode, respectively. The states between different modes indicate six transitions between three modes.

5.2. Modes and transitions

Both a load cell sensor and a full bridge of strain gauge sensor can detect the locomotion modes (sit, stand, and walk) and the corresponding transition states. However, compared with the load cell sensor, for the strain gauge sensor, more detailed transition information could be obtained. In Fig. 7(a), the sit-stand and stand-sit transition states were presented. During the sit-stand transition state, the signal amplitude of the strain gauge sensor is from negative to positive, which indicates that FS first occurs, and then RS does for subject 2. From the information, we can infer that when subject 2 wants to stand from sit mode, the lower leg flexes, and then heel strike occurs. However, for the load cell sensor, the signal amplitude is larger than 0, and detailed movement information of the sit-stand transition state cannot be expressed clearly. In Fig. 7(b), the signal amplitude decreases to negative and increases to about zero during the stand-walk transition state, from which we can infer that when subject 2 begins to walk from stand mode, the center of pressure is transferred to prosthetic forefoot, and then the prosthesis is lifted. In the walk-stand transition state, the signal amplitude remains positive, which means the center of pressure is the prosthetic rearfoot. In Fig. 7(c), the sit-walk and walk-sit transitions may not be realized directly. During the sit-walk transition state, the center of pressure is transferred from rearfoot to forefoot. It means that when subject 2 plans to walk, the lower leg flexes and stand, and then subject 2 starts to walk. In the same way, during the sit-walk transition state, when subject 2 plans to sit, subject 2 remains standing for a while, and then subject 2 sits down and flexes the lower leg. Therefore, the true sit-walk and walk-sit transitions are close to sit-stand-walk and walk-stand-sit transitions, respectively.

6. Discussion

6.1. Method comparison

Gait event detection for the wearable devices could be realized by different sensor systems. Referring to a gait partitioning review,[23] the characteristics of different sensor systems including our proposed method are listed in Table IV. Footswitches could sense the interaction-force change, which shows a good performance on cost, sensor placement, and signal post-processing. For example, Au *et al.* utilized six capacitive force transducers as footswitches, to detect the heel contact and toe contact.[7] Sup *et al.* utilized two full bridges of strain gauges as footswitches, to detect ball of foot contact and heel strike. But, due to the discrete signal from the footswitches (on/off), the sensor could not gain all possible granularities. In addition, this sensor needs to be improved in terms of service life. The pressure insoles can sense the interaction-force change, but the insoles have the same problems

https://doi.org/10.1017/S0263574719000390 Published online by Cambridge University Press

Table IV. Comparisons between different gait-event detection systems for the wearable devices.

Sensor system	**Sensor cost**[1]	**Service life**[2]	**Critical sensor placement**[2]	**All possible granularities** [3]	**Signal processing complexity**[4]	**Measurement object**[5]
Footswitches	Low	High	No	No	Low	Interaction force
Pressure insoles	Low	High	No	No	Low	Interaction force
IMUs	Low	High	Yes	Yes	Medium	Kinematics
Electromyograph	High	High	Yes	Yes	High	Neuromuscular activation
Load cell[6]	Medium	Low	Yes	No	Low	Interaction force
Proposed methods	High	High	No	Yes (Stance)	Low	Interaction force

IMU, Inertial measurement units. [1] "Sensor cost" indicator refers to average economic cost. This indicator has an effect on the commercial application. [2] "Service life" indicator refers to the ability that the sensor could be used in daily life. [3] "All possible granularities" indicator refers to whether the sensor has the ability to detect all possible gait events. [4] "Signal processing complexity" indicator refers to the algorithm complexity to realize the detection of gait events. [5] "Measurement object" indicator refers to the object that the original signals could measure and reflect. [6] The load cell sensor was installed between the adaptor and prosthetic socket. The net height and weight of this sensor is 8 mm and 90 g, respectively.

as the footswitches sensor. Inertial Measurement Units (IMUs) work by detecting linear acceleration and rotational rate, using a combination of one or more accelerometers and gyroscopes. Some also include a magnetometer to be used as a heading reference. To measure the space kinematics, typical configurations contain one accelerometer, gyroscope, and magnetometer per axis for each of the three axes. IMUs show some advantages of cost, service life, and detecting all possible granularities. However, to obtain the stable gait event, the sensor placement is critical, and usually some model prediction methods are utilized in signal post-processing to find the relationship between gait event and original signals.[23] Electromyograph could measure the muscle electronic signal from neuromuscular activation, which is a direct measurement method to detect motion intention. Due to high cost, critical sensor placement, and high post-signal processing, the electromyograph required to be improved. In our prior study, to distinguish the stance phase and the swing phase, the load cell sensor was installed between the adaptor and prosthetic socket.[11,12] To install the sensor, for the robotic prosthesis, the extra weight (90 g) and height (8 cm) are required. To obtain the stable signal, the sensor needed to be placed strictly in line with the center of adaptor and prosthetic socket. In addition, the sensor drift would occur due to material deformation (*e.g.* disc spring, bushing, and sealing rubber ring; see Fig. 1). In this paper, to deal with the limitations of the load cell sensor, we proposed a novel method to detect stance phase and swing phase through one full bridge of strain gauge. The sensor system could sense the interaction force between carbon-fiber foot and ground, and have some characteristics of low cost, high service life, no critical sensor placement, and low signal post-processing. In addition, one full bridge of strain gauge could sense all possible granularities during stance phase.

6.2. Possible future application

In this paper, the experimental results show that swing phase and stance phase can be estimated by a full bridge of strain gauge sensor. In addition, more detailed information on stance phase can be found. For example, for a full bridge of strain gauge sensor during stance phase, the signal amplitude is transferred from positive and negative values, which indicates that the center of pressure is transferred from rearfoot and forefoot. The dividing point between positive and negative values indicates that the center of pressure is transferred to the center of carbon-fiber footplate. For example, the minimum value (maximum negative value) reflects the maximum bending upward for the carbon-fiber footplate, which may indicate that push-off should occur at this moment and it can be useful to control the prosthesis. For different terrains and subjects, human locomotion shows different kinematics and kinetics.[11,12,20–22] In this paper, for different terrains and subjects, the full bridge of strain gauge sensor can measure the entire deformation of carbon-fiber footplate on different terrains during stance phase, shown in Figs. 6 and 7. Therefore, whether the signals from a full bridge of strain gauge sensor can detect terrains for each subject becomes a possible idea. To discuss the possibility of this idea, for the same subject, the sensor data on different terrains were plotted in one same figure, shown in Fig. 8. In Fig. 8, for subject 2, the maximum value during

https://doi.org/10.1017/S0263574719000390 Published online by Cambridge University Press

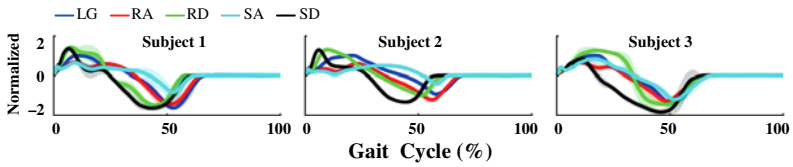


Fig. 8. The performance of a full bridge of strain gauge sensor at different terrains. The line and corresponding shape area refer to the mean and standard deviation. The abbreviations LG, RA, RD, SA, and SD stand for level ground, ramp ascent, ramp descent, stair ascent, and stair descent, respectively. The blue, red, green, cyan, and black lines refer to LG, RA, RD, SA, and SD, respectively.

stance phase for RD and SD is greater than the value for RA and SA, which indicates that subject 2 is used to RS first. While walking ascent (RA and SA), subject 2 is used to mid-foot strike first at the beginning of stance phase. The moment, when the curve occurs minimum value in one gait cycle, also shows some difference between different terrains. In addition, the ratio of swing phase to stance phase in one gait cycle shows some difference between different terrains. From the walking characteristics of different terrains, the terrain types could be inferred. Furthermore, based on the signals from a full bridge of strain gauge sensor, the corresponding methods of pattern recognition may be applied to terrain recognition. It is noted that there are different walking preferences between individuals. The difference between individuals needs to be considered. When the terrain types are determined, the prosthetic ankle kinematics and kinetics need to be changed, and the corresponding control parameters need to be adjusted.[11,12]

7. Conclusion

In this paper, we proposed a new method to detect gait events for a robotic prosthesis. This method utilized one full bridge of strain gauge sensor to measure the entire deformation of carbon-fiber footplate during stance phase. Three unilateral transtibial subjects volunteered to participate in the experiments. Five terrains (LG, RA/RD, and SA/SD) were studied. Experimental results show that the gait phases (stance phase and swing phase) can be estimated. The estimation accuracy is close to 100%. Based on gait events, two gait phases and three modes (sit, stand, and walk) were determined. Moreover, based on the detected gait phases and modes, a new control method was proposed. At last, the potential applications of this strain gauge sensor on detailed gait phase estimation and terrain detection and limitations of this paper were discussed. In the future, more works can focus on detailed gait phase detection and terrain detection using one full bridge of strain gauge sensor.

Acknowledgments

The authors would like to thank the anonymous reviewers for their valuable suggestions. This work was supported by the National Key R&D Program of China (No. 2018YFB1307302), the National Natural Science Foundation of China (No. 91648207, 61533001), and the National Program for Support of Top-notch Young Professionals. Q. Wang has commercial interests in Beijing SpeedSmart Co., Ltd., a spin-off company of Peking University. Currently, the IP protecting the prosthesis technology has been licensed to SpeedSmart Co. Ltd. for commercial exploitation.

References

1. D. A. Winter and S. E. Sienko, "Biomechanics of below-knee amputee gait," *J. Biomech.* **21**(5), 361–367 (1988).
2. N. H. Molen, "Energy/speed relation of below-knee amputees walking on motor-driven treadmill," *Int. Z Angew. Physiol.* **31**, 173–185 (1973).
3. J. Zhu, Q. Wang and L. Wang, "On the design of a powered transtibial prosthesis with stiffness adaptable ankle and toe joints," *IEEE Trans. Ind. Electron.* **61**(9), 4797–4807 (2014).
4. G. K. Klute, J. M. Czerniecki and B. Hannaford, "Artificial muscles: Actuators for biorobotic systems," *Int. J. Robot. Res.* **21**(4), 295–309 (2002).
5. J. Hitt, T. Sugar, M. Holgate, R. Bellman and K. Hollander, "Robotic transtibial prosthesis with biomechanical energy regeneration," *Ind. Rob.* **36**(5), 441–447 (2009).
6. F. Sup, H. A. Varol, J. Mitchell, T. J. Withrow and M. Goldfarb, "Preliminary evaluations of a self-contained anthropomorphic transfemoral prosthesis," *IEEE ASME Trans. Mechatron.* **14**(6), 667–676 (2009).

https://doi.org/10.1017/S0263574719000390 Published online by Cambridge University Press

7. S. K. Au, J. Weber and H. Herr, "Powered ankle-foot prosthesis improves walking metabolic economy," *IEEE Trans. Robot.* **25**(1), 51–66 (2009).
8. H. Herr and A. M. Grabowski, "Bionic ankle-foot prosthesis normalizes walking gait for persons with leg amputation," *Proc. Biol. Sci.* **279**, 457–464 (2012).
9. P. Cherelle, V. Grosu, A. Matthys, B. Vanderborght and D. Lefeber, "Design and validation of the ankle mimicking prosthetic (AMP-) foot 2.0," *IEEE Trans. Neural. Syst. Rehabil. Eng.* **22**(1), 138–148 (2014).
10. B. E. Lawson, J. Mitchell, D. Truex, A. Shultz, E. Ledoux and M. Goldfarb, "A robotic leg prosthesis: Design, control, and implementation," *IEEE Robot. Autom. Mag.* **21**, 70–81 (2014).
11. Q. Wang, K. Yuan, J. Zhu and L. Wang, "Walk the walk: A lightweight active transtibial prosthesis," *IEEE Robot. Autom. Mag.* **22**(4), 80–89 (2015).
12. Y. Feng and Q. Wang, "Combining push-off power and nonlinear damping behaviors for a lightweight motor-driven transtibial prosthesis," *IEEE ASME Trans. Mechatron.* **22**(6), 2512–2523 (2017).
13. E. Zheng, S. Manca, T. Yan, A. Parri, N. Vitiello and Q. Wang, "Gait phase estimation based on noncontact capacitive sensing and adaptive oscillators," *IEEE Trans. Biomed. Eng.* **64**(10), 2419–2430 (2017).
14. K. Kyoungchul and M. Tomizuka, "A gait monitoring system based on air pressure sensors embedded in a shoe," *IEEE ASME Trans. Mechatron.* **14**(3), 358–370 (2009).
15. A. Mannini, V. Genovese and A. M. Sabatini, "Online decoding of hidden Markov models for gait event detection using foot-mounted gyroscopes," *IEEE J. Biomed. Health Inform.* **18**(4), 1122–1130 (2014).
16. B. Chen, Q. Wang and L. Wang, "Adaptive slope walking with a robotic transtibial prosthesis based on volitional EMG control," *IEEE ASME Trans. Mechatron.* **20**(5), 2146–2157 (2015).
17. K. Yuan, Q. Wang and L. Wang, "Energy-efficient braking torque control of robotic transtibial prosthesis," *IEEE ASME Trans. Mechatron.* **22**(1), 149–160 (2017).
18. E. Zheng and Q. Wang, "Noncontact capacitive sensing-based locomotion transition recognition for amputees with robotic transtibial prostheses," *IEEE Trans. Neural. Syst. Rehabil. Eng.* **25**(2), 161–170 (2017).
19. S. Özyürek, İ. Demirbüken and S. Angın, "Altered movement strategies in sit-to-stand task in persons with transtibial amputation," *Prosthet. Orthot. Int.* **4**(38), 303–309 (2014).
20. R. Riener, M. Rabuffetti and C. Frigo, "Stair ascent and descent at different inclinations," *Gait Posture* **15**, 32–44 (2002).
21. A. N. Lay, C. J. Hass and R. J. Gregor, "The effects of sloped surfaces on locomotion: A kinematic and kinetic analysis," *J. Biomech.* **39**, 1621–1628 (2006).
22. M. R. Samantha, R. B. Graham and P. A. Costigan, "Differentiation of young and older adult stair climbing gait using principal component analysis," *Gait Posture* **31**, 197–203 (2010).
23. J. Taborri, E. Palermo, S. Rossi and P. Cappa, "Gait partitioning methods: A systematic review," *Sensors* **16**(1), 66 (2016).

https://doi.org/10.1017/S0263574719000390 Published online by Cambridge University Press